

POLARIZATION INSENSITIVE QUASI-PHASE-MATCHED SECOND HARMONIC GENERATION

XIAO-SHI SONG, QIN WANG, ZI-YAN YU, FEI XU
and YAN-QING LU*

*College of Engineering and Applied Sciences and
National Laboratory of Solid State Microstructures,
Nanjing University, Nanjing 210093, China
yqlu@nju.edu.cn

Received 16 May 2011

Polarization insensitive second harmonic generation (SHG) is proposed in an electro-optic (EO) tunable periodically poled Lithium Niobate (PPLN). The PPLN consists of four sections. External electric fields could be selectively applied to them to induce polarization rotation between the ordinary and extraordinary waves. If the domain structure is well-designed, the fundamental wave with an arbitrary polarization state can be frequency doubled efficiently in this special PPLN.

Keywords: Quasi phase matching; polarization insensitive; second harmonic generation; electro-optic effect.

1. Introduction

In the past decades, great research attention has been paid to nonlinear optical materials and devices. In addition to the conventional frequency conversion for various lasers, nonlinear optics also plays an important role in classical and quantum information processing, such as all-optical switching^{1,2} and single photon detection.^{3,4} We know that efficient frequency conversion demands a velocity matching among the interacting optical waves. This condition is not naturally satisfied owing to material dispersion. The birefringence phase matching⁵ technique is normally used for certain polarization states at a limited wavelength and temperature range. The nonlinear crystal should be well-orientated along a specific direction. As a result, the nonlinear optical interactions are polarization sensitive, namely, if the polarization state of the light source is uncertain, the output light power may vary severely. Sometimes the efficiency could even decline to zero, which restricts the applications of nonlinear information optics. For example, if the input light comes from an optical fiber, any pressure or disturbance on the fiber may influence the

*Corresponding author.

light polarization dramatically. Therefore it is much desired to suppress the polarization dependency for nonlinear optical processes.

On the other hand, artificial photonic microstructures have been hot topics for years in the optics community, such as photonic crystals⁶ and metamaterials.⁷ They may have some properties that do not exist in normal homogeneous materials. Quasi-phase-matched (QPM) materials are good examples among them,^{1,8–10} which are also called nonlinear photonic crystals.⁸ As a consequence, it is natural to pursue polarization insensitive frequency conversion in microstructured nonlinear materials. This would be a topic that has both fundamental research interests and important technical applications.

In this paper, a four-section periodically poled LiNbO₃ (PPLN) is proposed to realize the polarization insensitive second harmonic generation (SHG). External DC electric fields along the y -axis are applied to given PPLN parts.¹¹ The period of each PPLN section should be well-designed to either satisfy the quasi-phase-matching (QPM) condition or induce a polarization rotation for involved lights. We demonstrated that the SHG could be realized efficiently even though the fundamental wave (FW) has an arbitrary state of polarization. The interaction among these waves is investigated through coupling wave equations. The related mechanism and future applications are also discussed.

2. Model and Theoretical Simulation

Figure 1 shows the schematic diagram of a polarization insensitive PPLN containing four sections. The first and the fourth sections are identical, whose period is designed just for QPM SHG. The second and the third sections are for polarization rotation of the FW and the second harmonic (SH), respectively. External DC electrical fields are applied at the y -surfaces of the second and third sections of the sample.¹¹ In order to utilize the largest nonlinear coefficient d_{33} of LiNbO₃, the lights should propagate along the x -axis of this PPLN.

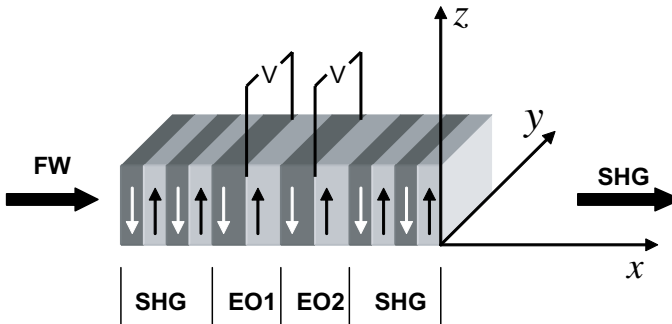


Fig. 1. Schematic diagram of a four-section PPLN. External electric fields are applied along the y -axis at the second and the third sections, represented with EO1 and EO2 in the figure.

When a z -polarized FW is propagated through the sample, part of the FW will be converted to the z -polarized SH in the first section, and then the generated z -polarized SH will be further converted to a y -polarized SH in the third section. The left z -polarized FW leaving from the first section is converted to y -polarized FW, so they are not able to be further doubled in the last section. On the other hand, when a y -polarized FW is injected and passes through section 1, it will be converted to a z -polarized wave in the second section, and then the generated z -polarized FW will be frequency doubled to a z -polarized SH in the fourth section. In other words, a y -polarized FW generates a z -polarized SH while a z -polarized FW results in a y -polarized SH. As long as the first and the last sections have the same length, the PPLN may have the same SHG capability for y - and z -polarized FWs. Because all normally-incident lights could be divided into y - and z -polarized components, polarization insensitive frequency doubling could therefore be expected.

To analyze the above processes in detail and obtain the numerical results, the corresponding coupling equations can be deduced under the plane-wave approximation, with consideration of both SHG and electro-optic (EO) interactions.^{12,13}

$$\left\{ \begin{array}{l} \frac{dE_{1y}}{dx} = -i \frac{\omega_1}{n_{1y}c} \varepsilon_{23}^{(1)}(x) E_{1z} e^{i\Delta k'_1 x} \\ \frac{dE_{1z}}{dx} = -i \frac{\omega_1}{n_{1z}c} [\varepsilon_{23}^{(1)}(x) E_{1y} e^{-i\Delta k'_1 x} + d_{33}(x) E_{1z}^* E_{2z} e^{i\Delta k'_2 x}] \\ \frac{dE_{2y}}{dx} = -i \frac{\omega_2}{n_{2y}c} \varepsilon_{23}^{(2)}(x) E_{2z} e^{i\Delta k'_3 x} \\ \frac{dE_{2z}}{dx} = -i \frac{\omega_2}{2n_{2z}c} [2\varepsilon_{23}^{(2)}(x) E_{2y} e^{-i\Delta k'_3 x} + d_{33}(x) E_{1z}^2 e^{-i\Delta k'_2 x}] \end{array} \right. \quad (1)$$

where $E_{j\xi}$, $\omega_{j\xi}$, $k_{j\xi}$ and $n_{j\xi}$ (the subscripts $j = 1, 2$ refer to the FW and SH, respectively, $\xi = y, z$ represent the polarization) are the external field amplitudes, the angular frequencies, the wave-vectors and the refractive indices, respectively. c is the speed of light in vacuum. $\omega_2 = 2\omega_1$ is the doubled light frequency. $\varepsilon_{23}^{(1)}(x) = -n_{1y}^2 n_{1z}^2 \gamma_{51}(x) E$ and $\varepsilon_{23}^{(2)}(x) = -n_{2y}^2 n_{2z}^2 \gamma_{51}(x) E$, where $\gamma_{51}(x) = \gamma_{51} f(x)$ is the modulated EO coefficient in PPLN. As no field is applied in the first and the fourth sections, the corresponding E value is 0. $d_{33}(x) = d_{33} f(x)$ is the modulated nonlinear optical coefficient, and the asterisk denotes complex conjugation. $\Delta k'_2 = k_{2z} - 2k_{1z}$, $\Delta k'_1 = k_{1y} - k_{1z}$, $\Delta k'_3 = k_{2y} - k_{2z}$ are the wave vector mismatch for SHG and polarization rotation of FW and SH, respectively.

In a PPLN, the structure function $f(x)$ changes its sign from +1 to -1 periodically in different domains. It can be expanded as Fourier series, $f(x) = \sum_m g_m \exp(-iG_m x)$, where G_m are the reciprocal vectors and g_m are the amplitudes of the reciprocal vectors. Without loss of generality, the reciprocal vector G_1 (the subscript 1 is ignored hereinafter) is adopted to achieve the highest conversion efficiency. In the first and fourth sections, to compensate the nonlinear phase

mismatch, $G_{1,4}$ (here the second subscript represents which section the reciprocal vector is in) is adopted as $\Delta k'_2 = k_{2z} - 2k_{1z} = G_{1,4}$, and the wave vector mismatch becomes $\Delta k_2 = k_{2z} - 2k_{1z} - G_{1,4} = 0$ for SHG. In the same way, G_2 of the second section is adopted to compensate the phase mismatch for FW's polarization rotation as $\Delta k'_1 = k_{1y} - k_{1z} = G_2$ (i.e., $\Delta k_1 = k_{1y} - k_{1z} - G_2 = 0$). In the third section, G_3 compensates the phase mismatch for SH's polarization rotation as $\Delta k'_3 = k_{2y} - k_{2z} = G_3$ ($\Delta k_3 = k_{2y} - k_{2z} - G_3 = 0$). In these (quasi) phase matched situations, the coupling equations (1) can be simplified as:

$$\begin{cases} \frac{dA_{1y}}{dx} = iK_1 A_{1z} e^{i\Delta k_1 x} \\ \frac{dA_{1z}}{dx} = iK_1^* A_{1y} e^{-i\Delta k_1 x} - iK_2 A_{1z}^* A_{2z} e^{i\Delta k_2 x} \\ \frac{dA_{2y}}{dx} = iK_3 A_{2z} e^{i\Delta k_3 x} \\ \frac{dA_{2z}}{dx} = -\frac{i}{2} K_2 A_{1z}^2 e^{-i\Delta k_2 x} + iK_3^* A_{2y} e^{-i\Delta k_3 x} \end{cases} \quad (2)$$

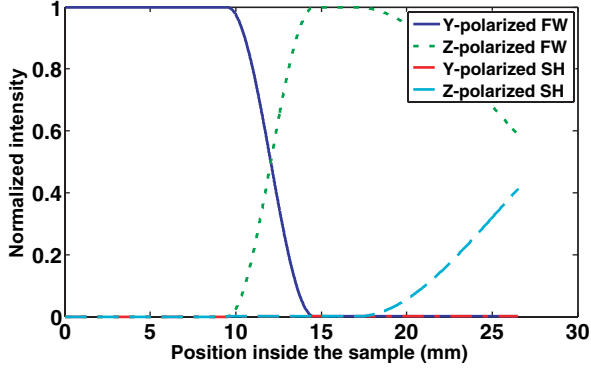
with

$$A_j = \sqrt{\frac{n_j}{\omega_j}} E_j, \quad K_1 = \frac{i\gamma_{51} g_1 \omega_1 E}{2c} \sqrt{n_{1y}^3 n_{1z}^3},$$

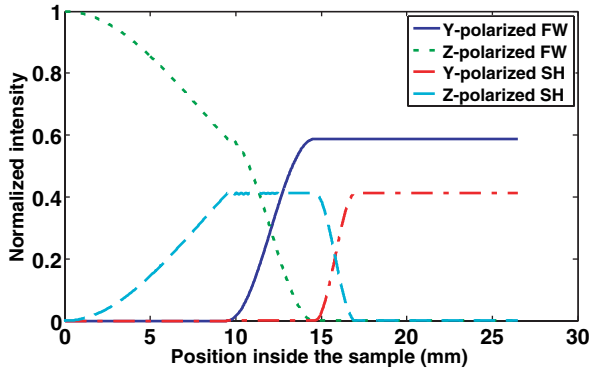
$$K_2 = \frac{g_1 d_{33}}{c} \sqrt{\frac{\omega_{1z}^2 \omega_{2z}}{n_{1z}^2 n_{2z}}}, \quad K_3 = \frac{i\gamma_{51} g_1 \omega_2 E}{2c} \sqrt{n_{2y}^3 n_{2z}^3}.$$

Numerical solutions to Eq. (2) are done to testify our design. We set the wavelength of FW at 1550 nm and working temperature T at 20°C. $\Lambda = 18.98 \mu\text{m}$ for the first and the fourth section with 500 periods in each one; $\Lambda = 20.48 \mu\text{m}$ for the second section and $\Lambda = 18.77 \mu\text{m}$ for the third section to satisfy the QPM and phase-matching conditions. $d_{33} = 25.2 \text{ pm/V}$, $\gamma_{51} = 32.6 \text{ pm/V}$ are employed for simulation. To realize a complete conversion between the ordinary and extraordinary waves, we set the external electric field at 710 V/mm and the periods of the second and third sections at 250 and 256 respectively. The pumping FW intensity is set at 2 MW/cm², which is much lower than the crystal's optical damage threshold.

Figures 2 and 3 show the simulation results. Figure 2 describes the light intensity evolution inside this four-section PPLN sample. It can be seen that the frequency doubling is realized no matter what kind of polarization state of FW is injected. The conversion efficiency remains $\sim 41\%$ for both y - and z -polarizations, agreeing well with our discussion. Figure 3 shows the spectral response. Figures 3(a) and 3(b) correspond to the results when a y -polarized pumping FW is injected. Figures 3(c) and 3(d) correspond to the results when a z -polarized FW is injected. For instance, when a y -polarized pumping FW is injected, the SH intensity has a peak at 1550 nm according to our design, meaning that the original y -polarized FW transferred its power to z -polarized FW ($\sim 59\%$) and z -polarized SH ($\sim 41\%$) totally. However, if



(a)



(b)

Fig. 2. (Color online) Normalized light intensity at different positions inside the four-section PPLN when the pumping wave is y -polarized (a) or z -polarized (b). Solid, dotted, dash-dotted and dashed curves represent y -polarized FW, z -polarized FW, y -polarized SH and z -polarized SH, respectively.

the wavelength has a small offset from the phase matching point, the SHG efficiency in the first and last sections drops quickly, while the y -to- z FW polarization rotation has wider wavelength bandwidth due to our design. A double-peak z -polarized FW spectrum is thus obtained at 1549 nm and 1551 nm. The results are similar when a z -polarized pumping wave is adopted.

In comparison with a normal PPLN, our sample has the same frequency doubling capability for y - and z -polarized FWs, but the efficiency is not as good as that of a normal PPLN. This is because some of the PPLN section is used for EO process rather than SHG. To evaluate our technique, the effective frequency-doubling coefficient d_{eff} is a suitable parameter.¹⁴ It is calculated to be 5.67 pm/V under small-signal approximation, which is lower than that of a normal PPLN, but is still larger than typical nonlinear crystals such as BBO and LBO.

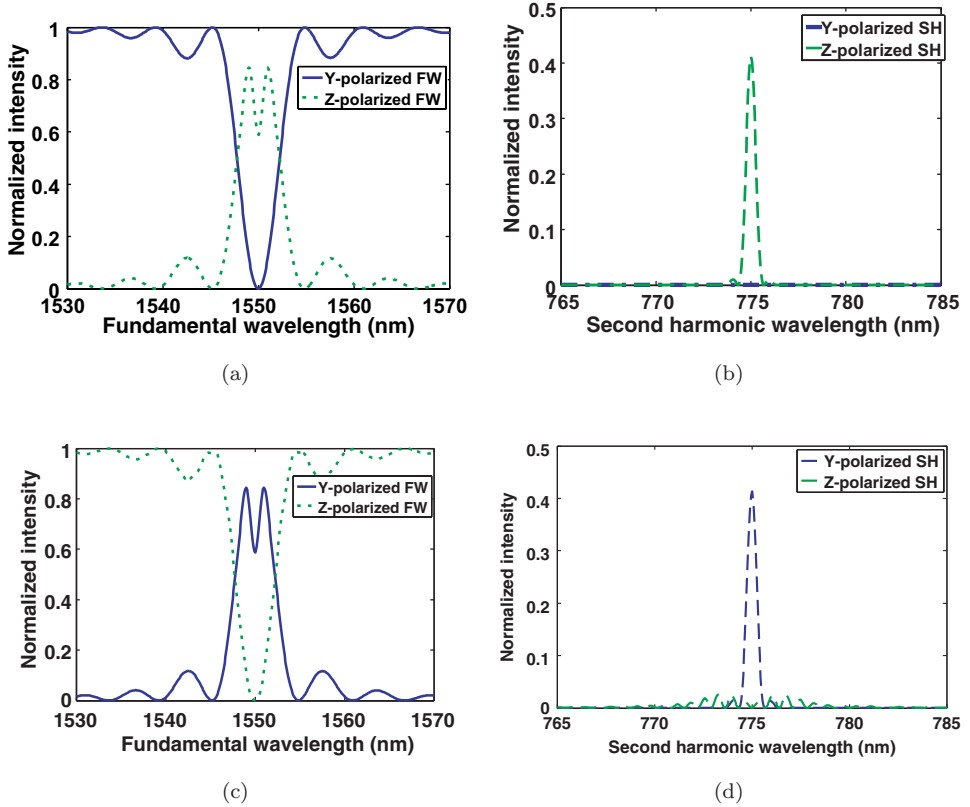


Fig. 3. (Color online) Normalized light intensity versus the wavelength when the FW is y -polarized ((a) and (b) correspond to FW and SH respectively) or z -polarized ((c) and (d) correspond to FW and SH respectively).

To fully investigate the PPLN’s polarization dependency, pure y - and z -polarized FWs are still lacking. The ratio between y - and z -polarized light field intensity and their phase difference are both important parameters. Figure 4 shows the simulation result about the conversion efficiency at different FW polarization states. It can be seen that when the ratio of the y -polarized FW intensity to the z -polarized FW intensity is settled, the conversion efficiency is basically unchangeable at arbitrary phase angles between y - and z - polarized lights. However, the conversion efficiency varies a lot along with the intensity ratio between the y - and z -polarized FWs. That is because the intensity of the generated SH is proportional to the square of the corresponding z -polarized FW intensity under small-signal approximation.¹⁵ If the pumping wave contains both z -polarized and y -polarized components, the generated SH intensity is less than the case when only a z -polarized or y -polarized pumping wave is injected. From Fig. 4, if the incident light is along the z -axis, the total SHG efficiency is 41%, as is already shown in Fig. 2. However, if the light intensity is equally distributed in y - and z -polarized components, the total

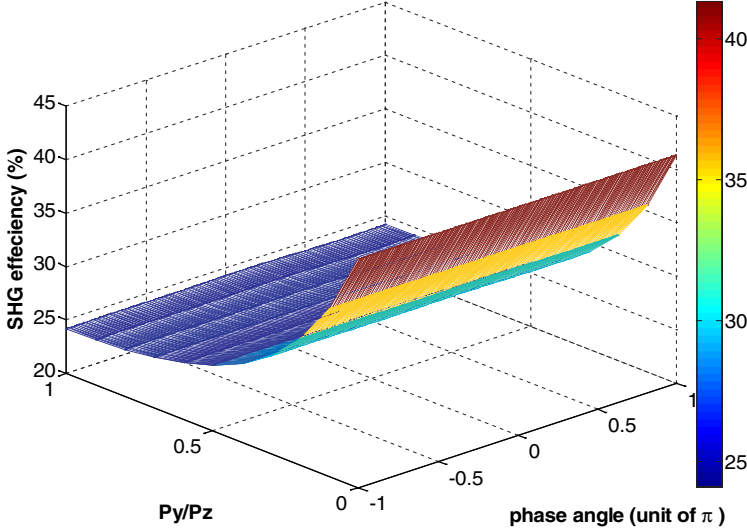


Fig. 4. (Color online) The SHG conversion efficiencies at arbitrary polarization states.

conversion efficiency is 24%, corresponding to the case with lowest efficiency. If the input FW power changes, the SHG efficiency changes accordingly, but the pure y - or z -polarized light always has the best results.

3. Discussion and Conclusion

Although our four-section PPLN still shows polarization dependency, its advantage is clear: as long as the FW is gathered into this monolithic crystal, efficient SHG could be realized at the phase-matching condition. The SH's polarization state is fully determined by the incident FW. Actually, this approach could be extended to other nonlinear processes such as difference frequency generation (DFG) and sum-frequency generation (SFG).¹ Applications in optical signal processing, fiber-optic communication and weak infrared light detection are expected.

In summary, we proposed a four-section PPLN that may greatly suppress the polarization sensitivity in nonlinear optical processes. An external electric field is applied to part of the PPLN to regulate the polarization states of FW and SH. In this case, a y -polarized pumping FW generates a z -polarized SH and a z -polarized FW contributes a y -polarized SH with the same efficiency. However, our PPLN still exhibits some polarization-dependency for FWs with arbitrary polarization states. The extensions and applications of this multi-section EO assisted PPLN scheme are also discussed.

Acknowledgments

This work is supported by National 973 program under contract No. 2011CBA00200 and 2010CB327800, NSFC program No. 60977039 and 10874080. The authors also

acknowledge the support from the Specialized Research Fund for the Doctoral Program of Higher Education.

References

1. Y. L. Lee, B. A. Yu, T. J. Eom, W. Shin, C. Jung, Y. C. Noh, J. Lee, D. K. Ko and K. Oh, All-optical AND and NAND gates based on cascaded second-order nonlinear processes in a Ti-diffused periodically poled LiNbO₃ waveguide, *Opt. Exp.* **14** (2006) 2776–2782.
2. C. J. Min, P. Wang, C. C. Chen, Y. Deng, Y. H. Lu, H. Ming, T. Y. Ning, Y. L. Zhou and G. Z. Yang, All-optical switching in subwavelength metallic grating structure containing nonlinear optical materials, *Opt. Lett.* **33** (2008) 869–871.
3. X. R. Gu, K. Huang, Y. Li, H. F. Pan, E. Wu and H. P. Zeng, Temporal and spectral control of single-photon frequency upconversion for pulsed radiation, *Appl. Phys. Lett.* **96** (2010) 131111.
4. H. Kamada, M. Asobe, T. Honjo, H. Takesue, Y. Nishida, O. Tadanaga and H. Miyazawa, Efficient and low-noise single-photon detection in 1550 nm communication band by frequency upconversion in periodically poled LiNbO₃ waveguides, *Opt. Lett.* **33** (2008) 639.
5. P. D. Maker, R. W. Terhune, M. Nisenoff and C. M. Savage, Effects of dispersion and focusing on the production of optical harmonics, *Phys. Rev. Lett.* **8** (1962) 21.
6. E. Yablonovitch, Inhibited spontaneous emission in solid-state physics and electronics, *Phys. Rev. Lett.* **58** (1987) 2059–2062.
7. A. Sihvola, Metamaterials in electromagnetics, *Metamaterials* **1** (2007) 2–11.
8. V. Berger, Nonlinear photonic crystals, *Phys. Rev. Lett.* **81** (1998) 4136–4139.
9. Y. Q. Lu, Y. Y. Zhu, Y. F. Chen, S. N. Zhu, N. B. Ming and Y. J. Feng, Optical properties of an ionic-type phononic crystals, *Science* **284** (1999) 1822.
10. K. Gallo, G. Assanto, K. R. Parameswaran and M. M. Fejer, All-optical diode in a periodically poled lithium niobate waveguide, *Appl. Phys. Lett.* **79** (2001) 314–316.
11. Y. Q. Lu, Z. L. Wan, Q. Wang, Y. X. Xi and N. B. Ming, Electro-optic effect of periodically poled optical superlattice LiNbO₃ and its applications, *Appl. Phys. Lett.* **77** (2000) 3719–3721.
12. C. P. Huang, Q. J. Wang and Y. Y. Zhu, Cascaded frequency doubling and electro-optic coupling in a single optical superlattice, *Appl. Phys. B* **80** (2005) 741–744.
13. Y. Kong, X. F. Chen and Y. Xia, Competition of frequency conversion and polarization coupling in periodically poled lithium niobate, *Appl. Phys. B* **91** (2008) 479–482.
14. R. W. Boyd, *Nonlinear Optics* (Academic Press, Inc., USA, 2002), Chap. 2.
15. A. Yariv and P. Yeh, *Optical Waves in Crystals* (Wiley, New York, 1984), Chap. 12.